International Symposium of Research Students on Materials Science and Engineering
December 20-22, 2004, Chennai, India
Department of Metallurgical and Materials Engineering, Indian Institute of Technology Madras

COMPARISON OF EXPERIMENTAL AND FINITE ELEMENT RESULTS FOR ELASTIC-PLASTIC STRESS/STRAIN BEHAVIOUR OF NOTCHED SHAFT UNDER MULTIAXIAL LOADING

[1]T.Nimali Medagedara, [2]Upul S Fernando, [3]P.D. Sarath Chandra and [4]M.C.J. Medagedara

[1,3]Department of Mechanical Engineering,
Open University of Sri Lanka, Nugegoda, Sri Lanka.
[2]School of Engineering, Sheffield Hallam University,
Pond Street, Sheffield, S1 1WB, UK
[4]Macrotech Engineering Pvt. Ltd

ABSTRACT

Many engineering components and structures are subjected to multiaxial stresses and strains under service conditions. Most of the engineering components contain stress concentration features or notches. For such notched components, even when the remotely applied load is uniaxial, the local stress-strain state developed at the critical locations or notches (where fatigue failures are likely to occur) is usually multiaxial because of the constraint effect at the notch. Machine components can experience a complex state of stress because generally they are not of simple geometry or as a result of multiaxial stress field that develops due to the application of two or more loads, which can be applied either simultaneously or in sequence. This paper compares the elastic-plastic stress/strain behaviour of notched shaft obtained from experiments and finite element method for non-proportional loading.Cyclic deformation experiments have been performed using solid cylindrical specimens with a circumferential notch. The specimens were subjected to tension-torsion non-proportional loading. The load-strain behaviour at the notch root has been recorded. The tests have been performed for four different non-proportional loading histories. Similar results have been derived from the finite element method using ABAQUS software.The results show that the FE predicted load-strain hysteresis behaviour is comparable to the experimental results for non-proportional loading cases. A description of the experiments, numerical models and the results are given. A brief discussion on the non-proportional hysteresis behaviour of notched shaft is presented.

1. INTRODUCTION

The fatigue behaviour of an engineering component can be very difficult to resolve under multiaxial loading. In complex stress state the three principal stresses are non-proportional or their directions change during a loading cycle. Fatigue under these conditions, termed multiaxial fatigue.

In order to understand the cyclic deformation of carbon steel, fatigue test had been carried out under combined non-proportional loading. Tests were carried out using solid notched specimens at room temperature under displacement control for both torsion and tension loadings.
The strain amplitudes were measured by using strain gauges attached to the specimen at the notch root. They were connected to the amplifiers to measure the strains in three directions. The results predicted by Finite Element Analyses (ABAQUS Code) were compared with experimental results.

2. MATERIAL AND SPECIMEN CONFIGURATION

The material used was conventional industrial medium carbon steel, EN 8 (SAE Grade 1040) whose yield stress is 320 MPa and ultimate strength is 730 MPa. Maximum allowable notch diameter, length of the specimen and the other dimensions were calculated for the specimen in conformity with the testing machine specification. The tests were carried out on solid specimens, which have an outer diameter of 35mm, notch diameter of 15mm and notch root diameter of 10mm.

3. STRAIN MEASUREMENTS

Considering the Fig. 1, for axial loading,
$\varepsilon_1 = \varepsilon_x$, $\varepsilon_3 = -\nu\varepsilon_x$ and $\varepsilon_2 = \varepsilon_x (1-\nu)/2$
For torsion loading , $\varepsilon_1 = \varepsilon_3 = 0$ and $\varepsilon_2 = \gamma_{xy}/2$
For combined tension and torsion loading, $\varepsilon_1 = \varepsilon_x$, $\varepsilon_3 = \varepsilon_y$ and $\gamma_{xy} = 2\varepsilon_2 - \varepsilon_1 - \varepsilon_3$
For the research, rosette strain gauges were used to measure strain at the notch root. Gauges were arranged as in Fig. 1. The strain was determined in three different directions for tension and torsion combined loading. Zero 0^o angle was used to measure strain in ε_1 direction, 90^o angle was used to measure strain in ε_3 direction and 45^o angle was used to measure strain in ε_2 direction as indicated in Fig. 1. The amplifiers were used to condition the strains in three different directions.

4. SELECTED MULTIAXIAL PATHS

Fig. 2 shows the strain paths selected in the experiments. The axial load and torque wave paths for the biaxial testing machine were created according to these paths.

5. COMBINED AXIAL-TORSION NON-PROPORTIONAL LOADING

5.1 Path-A -90^0 out-of phase loads

As the Fig. 3, axial load wave pattern was observed to be similar to the imposed one but torsion wave pattern was a little different due to inaccuracies of load control.

5.2 FEA results for non-proportional loading Path-A

Table 1 shows the load set used for 90^0 out-of phase FEA Ref No. 400. Fig. 4(a) shows the axial stress against axial strain loops obtained from FEA and experimental results. Both loops show little plasticity and FEA results behave more elastically. But the elastic gradient was the same for both hysteresis loops.

Fig. 4(b) shows the shear stress against shear strain for Test No.300 and FEA Ref No. 400. The gradient of the elastic region was same. But the experimental loops have more plasticity as depicted by hysteresis loop.

6. NON-PROPORTIONAL LOADING PATH-B

The variations of applied torque against axial load for Path-B load cases (Table 1) are shown in Fig. 5(a). The variation shown in Fig. 5(a) is same for shear strain (γ) against axial strain (ε) for

the Path-B loading. Fig. 2 has indicated the desired loading path but the path followed by the material during loading was slightly different as seen from Fig. 5(a). Considering Fig. 5(b), axial load wave pattern was observed to be similar to the input load pattern to the machine but torsion wave pattern was slightly different.

6.1 Comparison between FEA and Experimental results: For non-proportional loading Path-B

Fig. 6(a) shows the axial stress against axial strain loops. Shapes of the both loops (FEA and Experiment) were similar. The elastic gradient of both the hysteresis loops were identical. Considering Fig. 6(b) for the shear stress-shear strain loops the elastic gradient was observed to be the same and both hysteresis loops have more plastic area.

7. NON-PROPORTIONAL LOADING PATH – C

Table 1, shows the different load sets used for non-proportional load Path-C and Fig. 20 shows the variation of torque against the axial load for Path-C load.

The variations of applied torque against axial load for two non-proportional load Path-C cases are shown in Fig. 7(a). The shape of the variation (Fig. 7(a)) is the same for shear strain (γ) against axial strain (ε) for the Path-C loading. Fig. 2 indicates the imposed loading path but the path followed by the material in the experiment is slightly different from that imposed to it as observed to it as Fig. 7(a).

Considering Fig. 7(b), axial load wave pattern was similar to the input wave pattern but torsion wave pattern was little different. This is something, which is uncontrollable phenomenon through out the research.

7.1Comparison between FEA and Experimental results for non-proportional loading Path-C

Fig. 8(a) shows the axial stress against axial strain loops and both loops have plasticity. The elastic gradient of both hysteresis loops were also the same. Considering Fig. 8(b), for the shear stress-shear strain loop displays more plasticity as depicted by hysteresis.

8. NON-PROPORTIONAL LOAD PATH-D

Table 1 shows the different load sets used for non-proportional load tests for Path-D and Fig. 9(a) shows the variation of torque against the axial load through out the wave applied.

The variation of applied torque against axial load for all Path-D load cases is shown in Fig. 9(a). The shape of the variation shown in Fig. 9(a) is expected to be same for shear strain (γ) against axial strain (ε) for the Path-D loading. Fig. 2 indicates the imposed loading path but the path followed by the material during loading was slightly different as shown in Fig. 9(b).

8.1 Comparison between FEA and Experimental results: For non-proportional loading Path-D.

Fig. 10(a) shows the axial stress against axial strain loops and both loops have plasticity. The elastic gradient of the both hysteresis loops were the same. Fig. 10(b), for the shear stress-shear strain loops have more plasticity as depicted by hysteresis loops. When analysing the loads of the Test No.330 and Test No. 430, the obtained hysteresis loops for experiment and FEA were found to be different but the elastic gradient was the same for both tests.

9. CONCLUSION

The behavior of hysteresis loops (cyclic deformation) for material EN8 carbon steel under different non-proportional loadings was studied using the Finite Element Analysis and the experimental results. Comparing the results of FEA and experimental data, it can be seen that the general shape of the hysteresis loops are similar. However, FEA results showed less plastic deformation as evident from the reduced area of hysteresis loop compared to the experiments. This may be due to the inaccuracies of the control unit. However, the results show significant difference between FEA and experimental results in hysteresis behaviour under non-proportional loading. From these observations it may be concluded that the non-proportional loading Path-C is more damaging and Path-A is least damaging in terms of fatigue life considering the plastic strain ranges. And also the software available in the market for fatigue life prediction can be assessed for the same multiaxial different non-proportional loadings by using strain histories.

10. REFERENCES

[1] Bannantine J., Comer J. and Handrock, 1990, Fundamentals of Metal Fatigue Analysis, Prentice Hall.

[2] Benham P.P., Crowford R.J. and Armstrong C.G., 1996, Mechanics of Engineering Materials, 2nd Edition, Longman Group, pp 463-544.

TABLES

Table 1. Details of the applied loads

Test /FEA Ref. No.	Loading path	Axial load (kN)	Torque (Nm)	$\Delta\varepsilon$	$\Delta\gamma$
	Path-A				
300	Exp.	70	170	0.0026	0.0014
400	FEA	50	100	0.0030	0.0029
	Path-B				
310	Exp.	70	170	0.0042	0.0027
410	FEA	50	100	0.0038	0.0035
	Path-C				
320	Exp.	70	170	0.0049	0.0025
420	FEA	50	100	0.0040	0.0055
	Path-D				
330	Exp.	70	170	0.0045	0.0035
430	FEA	50	100	0.0040	0.0050

FIGURES

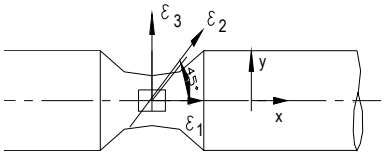

Fig. 1: Strain gauge position and direction

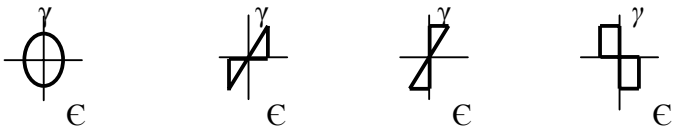

Out of phase - Path – A *Path – B* *Path - C* *Path - D*

Fig 2: Experimental strain paths

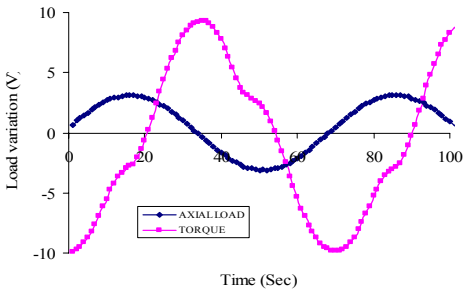

Fig. 3: Recorded axial load and torque variations with time for Test No. 300 in Table 1

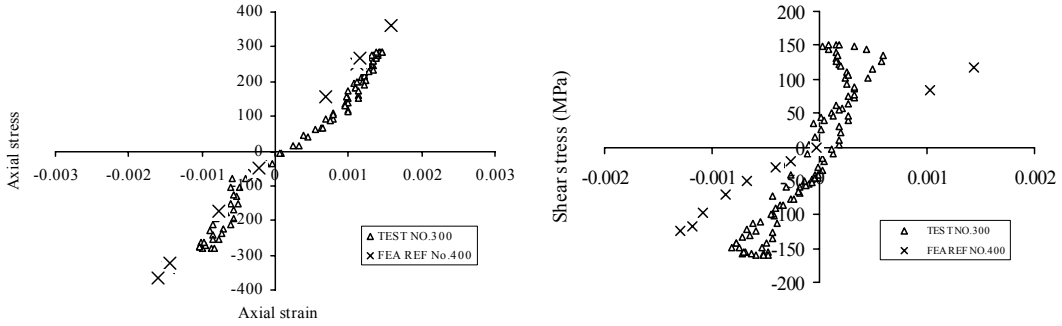

(a) (b)

Fig. 4: Axial stress vs axial strain and Shear stress vs shear strain for Test No. 300 and FEA Ref No. 400 in Table 1

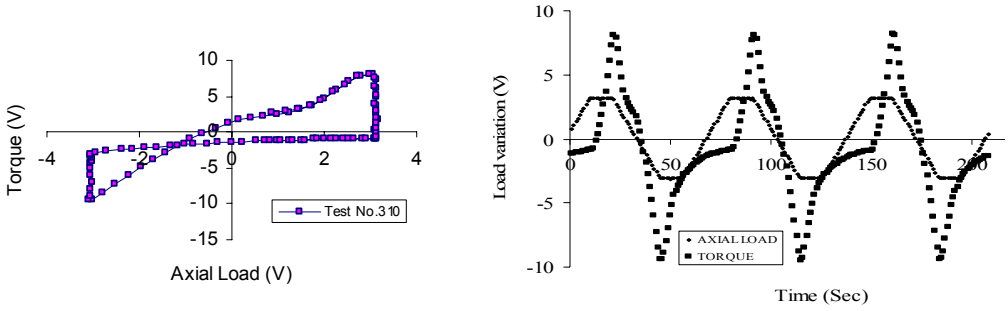

(a) (b)

Fig. 5(a) Variation of torque vs axial load and (b) Recorded axial load and torque variations with time for Path-B for load set 310

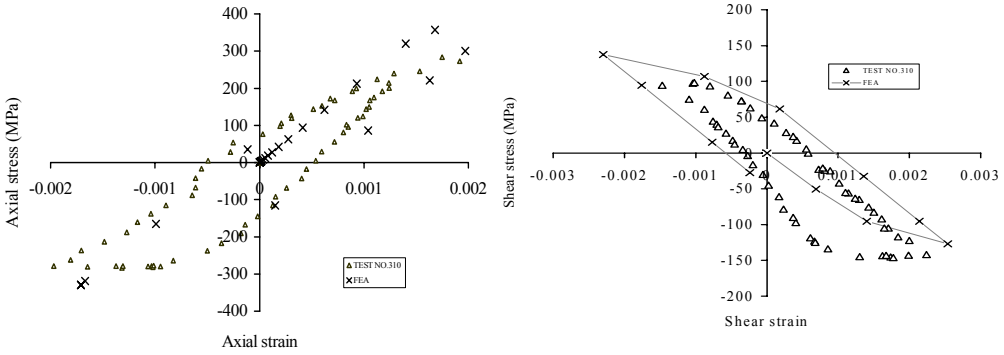

(a) (b)

Fig. 6: Comparison axial stress vs axial strain and shear stress vs shear strain for Test No. 310 and FEA Ref No. 410 in Table 1

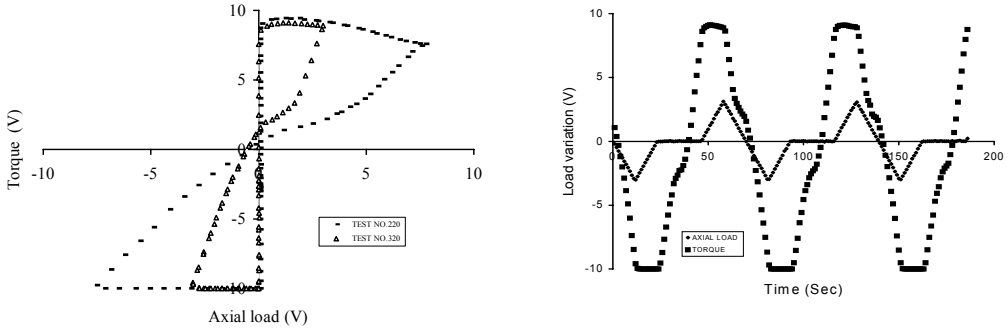

(a) (b)

Fig. 7: variation of applied torque vs applied axial load for Path-C

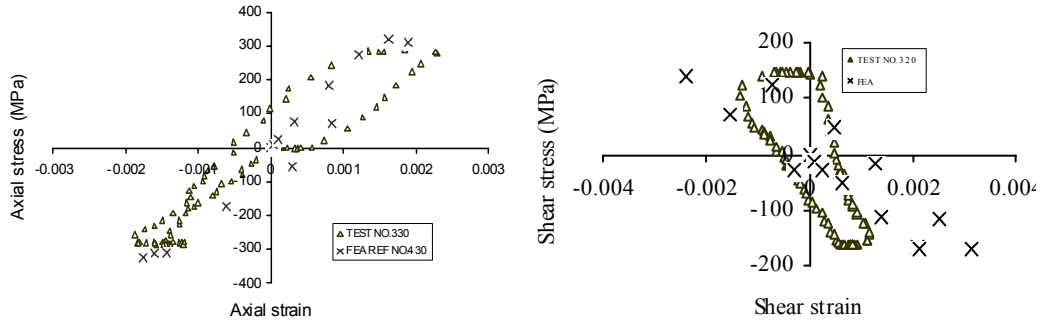

(a) (b)

Fig. 8: Comparison of axial stress vs axial strain for Test No. 320 and FEA Ref No. 420 in Table 3

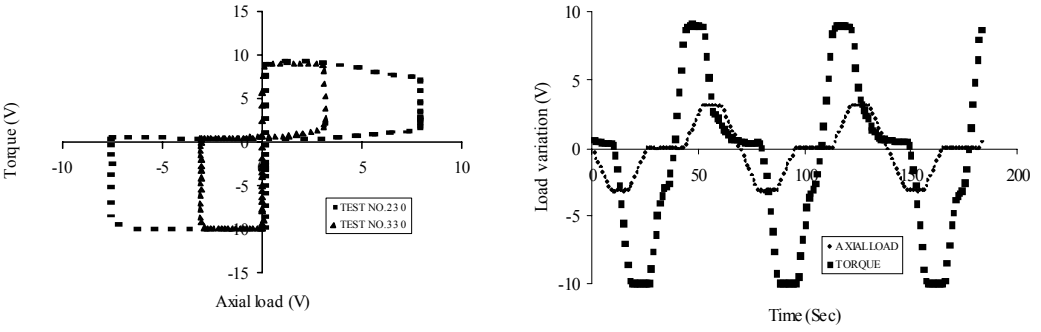

(a) (b)

Fig. 9:(a)Variation of torque vs axial load for Path-D (b) Recorded axial load and torque variation with time for Test No. 330 in Table1

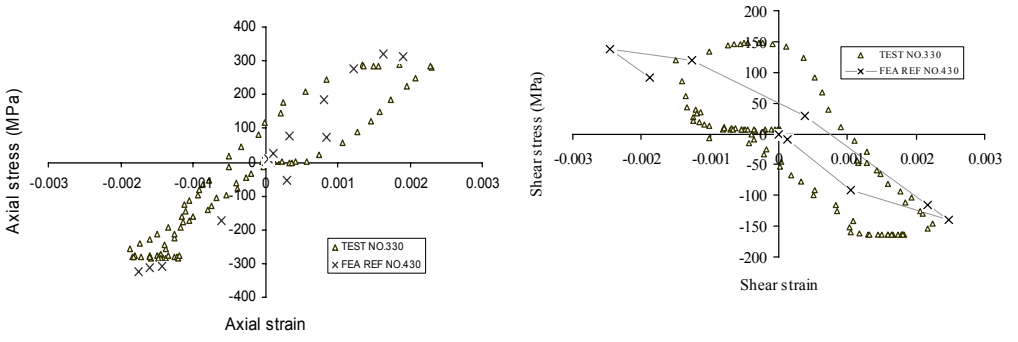

(a) (b)

Fig. 10:(a)Comparison axial stress vs axial strain (b Comparison shear stress vs shear strain for Test No. 330 and FEA Ref No. 430 in Table 1